Review Article　　　　**ISSN: 2394 - 658X**

Thermosolutale Convection in a Space Between an Elliptical plate and Horizontal plane: Influence of Mass Flux on the thermal and Dynamic Behavior of a Fluid

Fadel Diop, Alpha Malick Ndiaye, Omar Ngor Thiam and Cheikh Mbow

Fluid Mechanics, Hydraulics and Transfers Laboratory, Department of Physics, Faculty of science and Technology,
Cheikh Anta Diop University, Dakar, Senegal
fadeldiop1003@gmail.com
_____

ABSTRACT

This paper proposes to study unsteady natural convection in an enclosure bounded by a horizontal plane and a differentially heated elliptical wall. Using a conformal transformation, the curvilinear domain is reduced to a rectangular cross-section domain. The formulated transfer equations of the system such as: the equation of motion, heat and concentration are integrated using the finite volume method. The discretized equations are solved using the Thomas algorithm combined with a line-by-line iterative Gauss-Seidel scheme. The results of our study essentially concern the evolution of the temperature concentration and the current function to determine the behavior of the fluid in our domain by thermosolutal convection.Finally we will also look for the influence of the mass flow on the dynamic and thermal behavior of the fluid studied by setting the thermal Rayleigh number at 1.106 and taking for the mass Rayleigh number 0.100 and 1000.the results showed that the fulide is influenced by the mass flow for a mass Rayleigh number equal to 1000

Key words: elliptic-cylindrical coordinate system, finite volume method, isotherms, relaxation, unsteady natural convection, broadcast, concentration
_____

INTRODUCTION

Fluid flows confined in closed enclosures and mechanically or thermally entrained have been the subject of numerous theoretical, experimental and numerical studies as they are present in nature as well as in many industrial applications. They are used, for example, in turbomachinery, in lubrication, in the cooling of electronic components, in thermal ovens, in the deposition of substances on surfaces. On the fundamental level, closed enclosures offer a privileged framework for the study of thermoconvective instabilities and the exploration of the Roads to Chaos. Since the work of G. De Vahl Davis [1], many works have been devoted to thermal convection in cavities with rectangular [2], [3], [4] or cylindrical [5], [6] sections. In this respect, T. Kuehn and J. Goldstein [7] have carried out a rich investigation of natural convection in closed enclosures and have presented numerical and experimental results for different configurations over a wide range of Rayleigh and Prandtl numbers and geometric parameters. Thanks to the development of numerical tools, the authors have focused on flows in enclosures bounded by increasingly complex curvilinear boundaries and in annular spaces [8], [9], [10], [11]. The effects of Rayleigh (or Grashof) and Prandtl numbers as well as geometric parameters (eccentricity, form factor, tilt) on the thermal and dynamic fields have been studied. In 1994 U-Ch Shin et al [7] and in 1999 Z. Kabdi et al. in 1999 [8] numerically studied the two-dimensional natural thermal convection in cylindrical lunules with horizontal axis filled with air or enclosing a porous medium. The transfer equations written in the two-cylinder coordinate system were solved using the control volume method and the power law developed by Patankar [7]. The influence of the system parameters, notably the inclination with respect to the horizontal plane, the form factor, the modified Grashof number is studied. The average and local values of the Nusselt numbers as well as the distributions of the isotherms and current function lines are presented and

discussed. The minimum heat transfer is obtained for tilt angles between 30 and 45. For large values of the Grashof number, the transfer is accelerated and secondary flows occur. More recently, M. L. Sow et al [9] and M. N. Koïta et al [10] have numerically studied the effects of Rayleigh number, eccentricity and tilt on natural thermal convection in an annular space bounded by two vertically eccentric spheres. They showed that when the Rayleigh number reaches the value of 10^7, the flow becomes multicellular characterised by a state of pre-turbulence. They also showed that depending on the values of the eccentricity, the flow can change from a single-cell flow to a multi-cell flow. The common point from the mathematical modelling point of view of the works [8], [9], [10], [11] mentioned above is the use of conformal transformations which allows to reduce the physical domains to rectangular numerical domains. However, in these geometries, the poles, which are generally points of singularity, are located outside the study domain, and so the numerical study is facilitated. The natural convection in a domain delimited by a flat horizontal plate and a wall whose trace is a cylindrical half-ellipse has never, to our knowledge, been studied. The only case that resembles this geometrical configuration is the enclosure delimited by a flat wall and a cylindrical cap Z. Kabdi et al. in 1999 [3]. From a practical point of view, the cylindrical half-ellipse can be used as a deposition surface in thermally stable convection and it is interesting to study the uniform accessibility of such a surface. From a fundamental point of view it is to explore the thermoconvective instabilities in such a domain. This is why we propose in this paper to study the unsteady natural thermal convection in this closed enclosure in the elliptic-cylindrical coordinate system. One of the original features of our field of study, contrary to annular enclosures, is the presence of poles which are located on the plane surface

DESCRIPTION OF THE PROBLEM IN PHYSICAL DOMAIN

The physical domain in which we propose to study heat and momentum transfer within a fluid in an impermeable closed enclosure bounded by a half cylinder of equation

$$\left.\begin{array}{c} \left(\dfrac{x}{a_x}\right)^2 + \left(\dfrac{y}{a_y}\right)^2 = 1 \ ; \ \ y \geq 0 \\[2mm] \forall\, z \in [-l : +l] \end{array}\right\} \tag{1}$$

and a flat horizontal plate of width $(2.L)$ coinciding with the major axis of the ellipse and of depth $(2l)$ (Figure 1a). In our study we place ourselves in the case where a_x is the semi-major axis of the ellipse and we pose $a_x = L$

Initially the enclosure is filled with a fluid of density ρ_0 in thermodynamic equilibrium at temperature T_0 and thermally isolated from the external environment. The curvilinear boundary of the chamber is maintained at temperature T_0. We will assume hereafter that the depth of the enclosure $(2.l)$ is very large in front of the length of the major axis $(2.L)$.
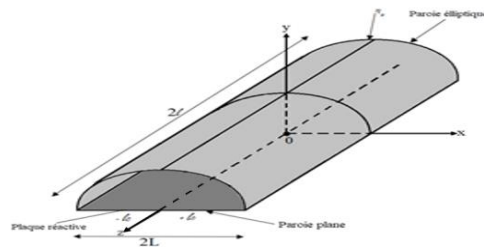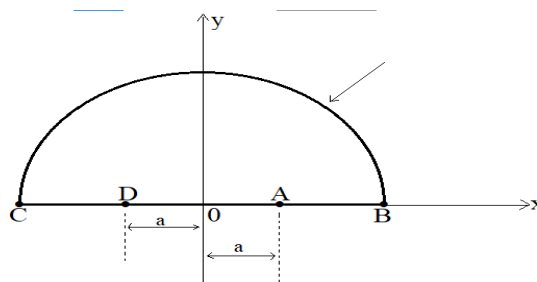

Fig.1a Schematic of the physical domain

Fig.1b Cross-section in the plane (z=0) of the physical domain

_____

Although it is simpler to write the equations modelling the transfers in a Cartesian (x, y)coordinate system, it is however more sensible to find a coordinate system in which the contours of our domain are constant coordinate surfaces. The shape of the curvilinear wall then led us to choose the elliptic-cylindrical coordinates (η, θ)which seem, naturally, to be the best suited to the geometry considered.

To generate the elliptic-cylindrical coordinates, we will use the following transformation

$$f(Z) = a.ch(Z) = a.ch(\eta + i.\theta) \qquad (3)$$

Hence

$$\left. \begin{array}{l} x = a.ch(\eta).cos(\theta) \\ y = a.sh(\eta).sin(\theta) \end{array} \right\} \qquad (4)$$

The (η)constants are ellipses with large axes $(2.a.ch\eta)$ and small axes $(2.a.sh\eta)$ while the (θ) constants are hyperbolas with asymptotes $y = x.\tan(\theta)$ and $y = -x.\tan(\theta)$.By translating the ellipses and hyperbolas along the horizontal axis (Oz), we then generate families of elliptical cylinders and hyperbolic sheets.

The size and shape of the elliptical domain are fixed by the values of η of the inner (η =0) and outer (η =η_p) ellipses while the θ coordinate varies between 0 and π. The flat plate portion ($y = 0$, $\forall z \in [-l : +l]$) is marked by

$$\begin{cases} \eta = 0 & \forall \theta \in [0 ; \pi] \\ \theta = 0 & \forall \eta \in [0 ; \eta_p] \\ & and \\ \theta = \pi & \forall \eta \in [0 ; \eta_p] \end{cases} \qquad (5)$$

Thus our curvilinear enclosure is transformed into a rectangular domain bounded by the coordinate lines (Figure2)

$$\eta = 0 \ et \ \eta = \eta_p \ ; \ \theta = 0 \ et \ \theta = \pi \ ; \ z = -l \ et \ z = +l$$
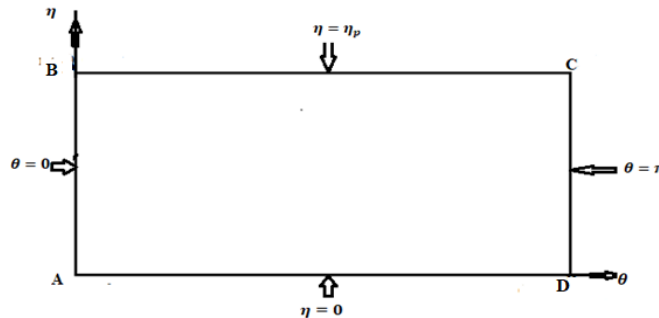

Fig.2 *Physical domain in the elliptic-cylindrical coordinate system. Section in the z=0 plane*

MATHEMATICAL FORMULATION

From an instant $T_0$the flat plate of the enclosure is heated to a constant temperature $T_p > T_0$. If the difference between the temperature of the fluid and that of the heated flat plate exceeds a certain threshold, the fluid then starts to move under the action of the non-uniformity of the density due to the temperature gradients in the domain. We propose to study the natural convection that will then arise in our enclosure under the following simplifying assumptions:

As $(2.L) \ll (2.l)$ then by placing ourselves very far from the vertical walls, we can consider that the transfers are plane and two-dimensional

The characteristic velocity of the flow is very small compared to the adiabatic sound velocity and therefore the powers of the pressure forces and the viscosity forces dissipated as heat are neglected compared to the other contributions in the enthalpy equation.

The fluid is transparent and the temperature differences are small enough that heat transfer by radiation can be neglected.

We assume that variations in the density of the fluid are taken into account only in the driving term of the Navier-Stokes equations and follow the following linear Boussinesq law

$$\rho = \rho_0[1 - \beta_T(T - T_0) + \beta_c(C - C_0)] \qquad (6)$$

Where $\beta_T = -\frac{1}{\rho_0}\left(\frac{\partial \rho}{\partial T}\right)_{c=cte}$ and $\beta_c = -\frac{1}{\rho_0}\left(\frac{\partial \rho}{\partial c}\right)_{T=cte}$ is the coefficient of thermal expansion.

_____

In natural convection the pressure field is not very interesting, especially when the powers of the pressure forces are neglected. To eliminate the pressure term, a substitution equation will have to be used by applying the rotational operator to both members of the equation of motion written in velocity-pressure variables. Since the flow is assumed to be plane and two-dimensional then the vorticity $\vec{\omega}$ and the potential vector $\vec{\psi}$ each have only one non-zero component which lies in the plane perpendicular to the flow plane. Therefore, positing $\vec{\omega} = \omega.\vec{e}_z$ and $\vec{\psi} = \psi.\vec{e}_z$. Thus using the current-vorticity function formalism then the equations governing the transfers are respectively vorticity equation; stream function equation; mass equation and heat equation

$$\frac{\partial \omega}{\partial t} + \vec{\nabla}.\left(\vec{v}.\omega - v.\vec{\nabla}\omega\right) = -\beta_T.\left(\vec{\nabla}\,T\right) \wedge \vec{g} \tag{7}$$

$$\vec{\nabla}.\left(-\vec{\nabla}\,\psi\right) = \omega \tag{8}$$

$$\frac{\partial c_i}{\partial t} + \vec{\nabla}.[\vec{v}.c_i] = \sum_{j=1}^{r}\gamma_{ij}.\varphi_j - \frac{1}{\rho}\vec{\nabla}.\left[\vec{J}(\rho_i)\right] + c_i.\left(\vec{\nabla}.\vec{v}\right) \tag{9}$$

$$\frac{\partial T}{\partial t} + \vec{\nabla}.\left(\vec{v}.T - \alpha.\vec{\nabla}T\right) = 0 \tag{10}$$

with $\vec{v}$, c, ω, ψ and T the velocity, concentration, vorticity, current function and temperature fields. v and α represent the kinematic viscosity coefficient and thermal diffusivity respectively.

 FORMULATION OF DIMENSIONLESS EQUATIONS IN CURVILINEAR COORDINATE SYSTEM
Given the multiplicity of parameters involved in the set of equations of our mathematical model, it would be useful to find a technique to reduce them. To do so, we can agglomerate them in the form of adimensional groupings having a physical meaning and which allow, among other things obtain information about the solution before solving the problem, to optimize a possible experimental approach.
By introducing the following reduced quantities

$$t^* = \frac{\alpha.t}{(a)^2}; \ \psi^* = \frac{\psi}{\alpha}; \ \omega^* = \frac{(a)^2.\omega}{\alpha}; \ T^* = \frac{T-T_0}{T_p - T_a}; \ C = c - c_0$$

The equations for the dimensionless current function, motion and heat projected onto the coordinate axes are
Dimensionless equation of the current function

$$-\frac{1}{h^{*2}}\left(\frac{\partial^2\psi^*}{\partial\eta^2} + \frac{\partial^2\psi^*}{\partial\theta^2}\right) = \omega^* \tag{11}$$

$$\frac{\partial\omega^*}{\partial t^*} + \frac{1}{h^{*2}}\left\{\frac{\partial}{\partial\eta}\left(h^*v_\eta^*\omega^* - Pr.\frac{\partial\omega^*}{\partial\eta}\right) + \frac{\partial}{\partial\theta}\left(h^*v_\theta^*\,\omega^* - Pr.\frac{\partial\omega^*}{\partial\theta}\right)\right\} = \frac{1}{h^{*2}}\left\{Bo.\left(\frac{\partial T^*}{\partial\eta}.sh\eta.cos\theta - \frac{\partial T^*}{\partial\theta}.ch\eta.sin\theta\right)\right\} \tag{12}$$

$$\frac{\partial C}{\partial t^*} + \vec{\nabla}^*.\left(\vec{v}.C - \frac{1}{Le}.\vec{\nabla}^*C\right) = 0 \tag{17}$$

$$\frac{\partial T^*}{\partial t^*} + \frac{1}{h^{*2}}\left\{\frac{\partial}{\partial\eta}\left(h^*v_\eta^* - \frac{\partial T^*}{\partial\eta}\right) + \frac{\partial}{\partial\theta}\left(h^*v_\theta^*T^* - \frac{\partial T^*}{\partial\theta}\right)\right\} = 0 \tag{13}$$

$$h = \sqrt{g_{ii}} = a.\sqrt{(ch\eta)^2 - (cos\theta)^2}$$

$$Pr = \frac{v}{\alpha} \ and \ \ Bo = Ra.Pr = \frac{\beta.g.(T_p - T_a).a^3}{\alpha^2} \ and$$

where Ra is the Rayleigh number.
We complete this system of equations with the following initial and boundary conditions
- **Initial condition**
  $$\psi^*(\eta,\theta\,;t^*=0) = \omega^*(\eta,\theta\,;t^*=0) = C(\eta,\theta) = T^*(\eta,\theta\,;t^*=0) = 0 \tag{14}$$

- **On the elliptical wall**: $\eta = \eta_p$; $\forall\theta \in \ ]0\,;\pi[$
  $$\psi^*\left(\eta_p,\theta;t^*\right) = T^*\left(\eta_p,\theta\,;t^*\right) = \frac{\partial C}{\partial\eta} = 0\ ;\ \omega^*\left(\eta_p,\theta;t^*\right) = -\frac{1}{h^{*2}}\frac{\partial^2\psi^*}{\partial\eta^2}\ ; \tag{15}$$

- **On the part of the flat plate**: $\eta = 0$; $\forall\theta \in \ ]0\,;\pi[$
  $$\psi^*(0,\theta\,;t^*) = 0;\ T^*(0,\theta\,;t^*) = 1;\ \frac{\partial C}{\partial\eta} = \pm Da.h^*.C;\ \omega^*(0,\theta\,;t^*) = -\frac{1}{h^{*2}}\frac{\partial^2\psi^*}{\partial\eta^2} \tag{16}$$

- **On the part of vertical plate:**

For $\theta = 0$; $\forall \eta \in \,]0 \, ; \eta_p[$

$$\psi^*(\eta, 0; t^*) = \frac{\partial C}{\partial \theta} = 0 \; ; \; \omega^*(\eta, 0; t^*) = -\frac{1}{h^{*2}} \frac{\partial^2 \psi^*}{\partial \theta^2} \text{ et } T^*(\eta, 0; t^*) = 1 \tag{17}$$

For $\theta = \pi$; $\forall \eta \in \,]0 \, ; \eta_p[$

$$\psi^*(\eta, \pi \, ; t^*) = \frac{\partial C}{\partial \theta} = 0 \; ; \omega^*(\eta, \pi \, ; t^*) = -\frac{1}{h^{*2}} \frac{\partial^2 \psi^*}{\partial \theta^2} \text{ et } T^*(\eta, \pi \, ; t^*) = 1 \tag{18}$$

Dimensionless connection conditions at points A, B, C and D
These points present discontinuities of the first kind, which forces us to approximate certain quantities at these points. We will have

- **To the point $A(\eta = 0 \, , \theta = 0)$**

$$\left.\frac{\partial \omega^*}{\partial \eta}\right|_{\theta=0} = -\left.\frac{\partial \omega^*}{\partial \theta}\right|_{\eta=0} \; ; \; \left.\frac{\partial C}{\partial \eta}\right|_{\eta=0} = \left.\frac{\partial C}{\partial \theta}\right|_{\theta=0} \tag{19}$$

- **To the point $D(\eta = 0 \, , \theta = \pi)$**

$$\left.\frac{\partial \omega^*}{\partial \eta}\right|_{\theta=\pi} = \left.\frac{\partial \omega^*}{\partial \theta}\right|_{\eta=0} \; ; \; \left.\frac{\partial C}{\partial \eta}\right|_{\eta=0} = \left.\frac{\partial C}{\partial \theta}\right|_{\theta=0} \tag{20}$$

- **To the point $B(\eta = \eta_p \, , \theta = 0)$**

$$\left.\frac{\partial T^*}{\partial \theta}\right|_{\eta=\eta_p} = \left.\frac{\partial T^*}{\partial \eta}\right|_{\theta=0} \tag{21}$$

$$\psi^*(\eta = \eta_p, \theta = 0 \, ; t^*) = \omega^*(\eta = \eta_p, \theta = 0 \, ; t^*) = 0$$

$$\left.\frac{\partial C}{\partial \theta}\right|_{\eta=\eta_p} = \left.\frac{\partial C}{\partial \eta}\right|_{\theta=0} \; ; \; \left.\frac{\partial \omega^*}{\partial \eta}\right|_{\eta=\eta_p} = \left.\frac{\partial \omega^*}{\partial \theta}\right|_{\theta=0} \tag{22}$$

- **To the point $C(\eta = \eta_p \, , \theta = \pi)$**

$$\left.\frac{\partial T^*}{\partial \theta}\right|_{\eta=\eta_p} = -\left.\frac{\partial T^*}{\partial \eta}\right|_{\theta=\pi} \tag{23}$$

$$\psi^*(\eta = \eta_p, \theta = \pi \, ; t^*) = \omega^*(\eta = \eta_p, \theta = \pi \, ; t^*) = 0$$

$$\left.\frac{\partial C}{\partial \theta}\right|_{\eta=\eta_p} = -\left.\frac{\partial C}{\partial \eta}\right|_{\theta=\pi} \; ; \; \left.\frac{\partial \omega^*}{\partial \eta}\right|_{\eta=\eta_p} = -\left.\frac{\partial \omega^*}{\partial \theta}\right|_{\theta=\pi} \tag{24}$$

Relationships (23) and (24) reflect the continuity of vorticity and heat flux.

NUMERICAL FORMULATION

The continuous domain (D) is reduced to a discrete domain consisting of elementary volumes $\delta \mathcal{V}_c$ called "control volumes". In order to avoid some unrealistic solutions, a shifted constant-step mesh is used in which the scalar fields are computed at the centre of the control volume P and the velocity components are evaluated at the centres of the facets marked by the indices e,n,w and s of the control volume (see Figures 3. b).
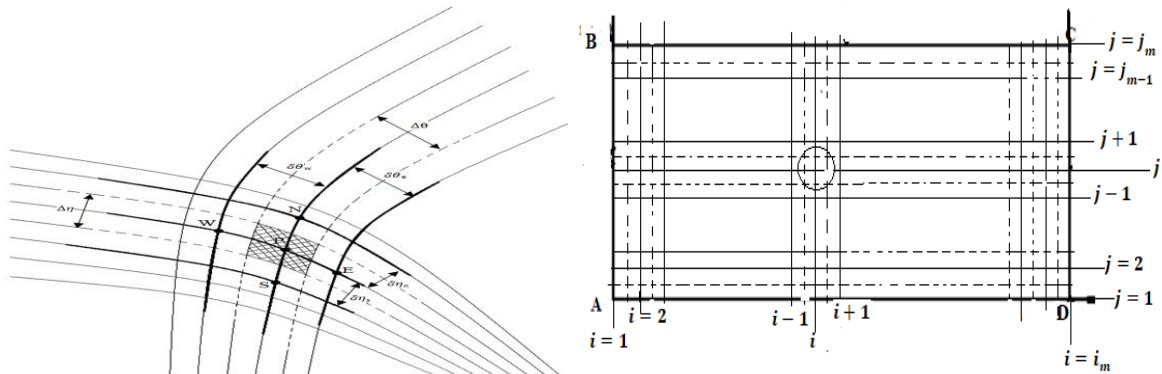

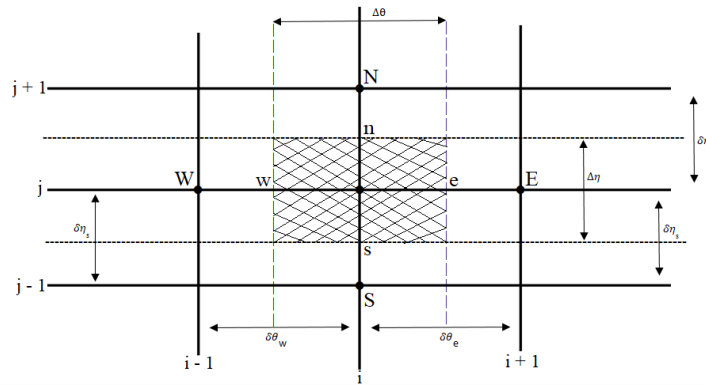***Fig.3a*** *Diagram of the mesh in the (x, y) plane*

***Fig.3b** Mesh diagram in the (η, θ) plane*

The equations are discretised using the Power Law Scheme [Patankar S. K., 1981; Perron S., 2001; Versteeg H. K., Malalasekera W., 1995]. The components of the velocities at the facets of the generic control volume are expressed in terms of the first derivatives of the current function whose values are calculated only at the centres of the control volumes. The Neumann-type boundary conditions are approximated by a decentred scheme of order two

An implicit two-layer Euler-type scheme with constant time step is used to approximate the time derivatives of the quantities. The resulting systems of equations are solved by an iterative over-relaxation method.

The process is stopped when the following convergence criterion is met

$$\frac{\sum_{i=1}^{i=i_m} |(\bar{\mathcal{F}}_i)^{k+1} - (\bar{\mathcal{F}}_i)^k|}{\sum_{i=1}^{i=i_m} |(\bar{\mathcal{F}}_i)^{k+1}|} \leq \varepsilon_{\bar{\mathcal{F}}} \qquad (25)$$

In addition to the criterion of convergence of the iterative processes, we must also define a criterion for stopping the calculation program. We stop the calculations when, at large times, the variations of our functions between two consecutive instants are very small. In these conditions we take as stopping criterion

$$min\{e_\theta; e_C; e_\omega; e_\psi\} \leq Cr_{\bar{\mathcal{F}}} \qquad (26)$$

With

$$e_{\bar{\mathcal{F}}} = \frac{\sum_{i=1}^{i=i_m} |(\bar{\mathcal{F}}_i)^{n+1} - (\bar{\mathcal{F}}_i)^n|}{\sum_{i=1}^{i=i_m} |(\bar{\mathcal{F}}_i)^{n+1}|} \qquad (27)$$

RESULTS AND DISCUSSION

The following results are relative to a Prandtl number of 0.7 et un nombre de Rayleigh thermique fixe a 1.10^6 .nous allons chercher linfluence du flux massique sur le comportement dynamique et thermique du fluide en faisant varier le nombre de Rayleigh massique comme suit:Ram=0 Ram=100 et Ram=1000

Table 1: Values of the numerical parameters of the functions

	Values of the numerical parameters of the functions			
	Current function	concentration	vorticity	Temperature
$\varepsilon_{\bar{\mathcal{F}}}$	0.005	0,00001	0.0004	0.005
Relaxation factor	0.79	0,1	0.078	0.78

In all that follows we have taken $\eta_p = 1$

     a.   **Thermal field, current lines and iso concentration at variable times $Rat = 1.10^{+6}$ and $Ram = 0$**

Figures (4) represent the isotherms, iso-concentrations and streamlines for different ones for $Rat = 1.10^{+6}$ and Ram=0. We note that these figures show that the regime of flow is two-celled. The cell rotates in the trigonometric direction and on the right side it rotates in the opposite direction (the particles of the fluid move upwards under the action of the forces of Archimedes' buoyancy).
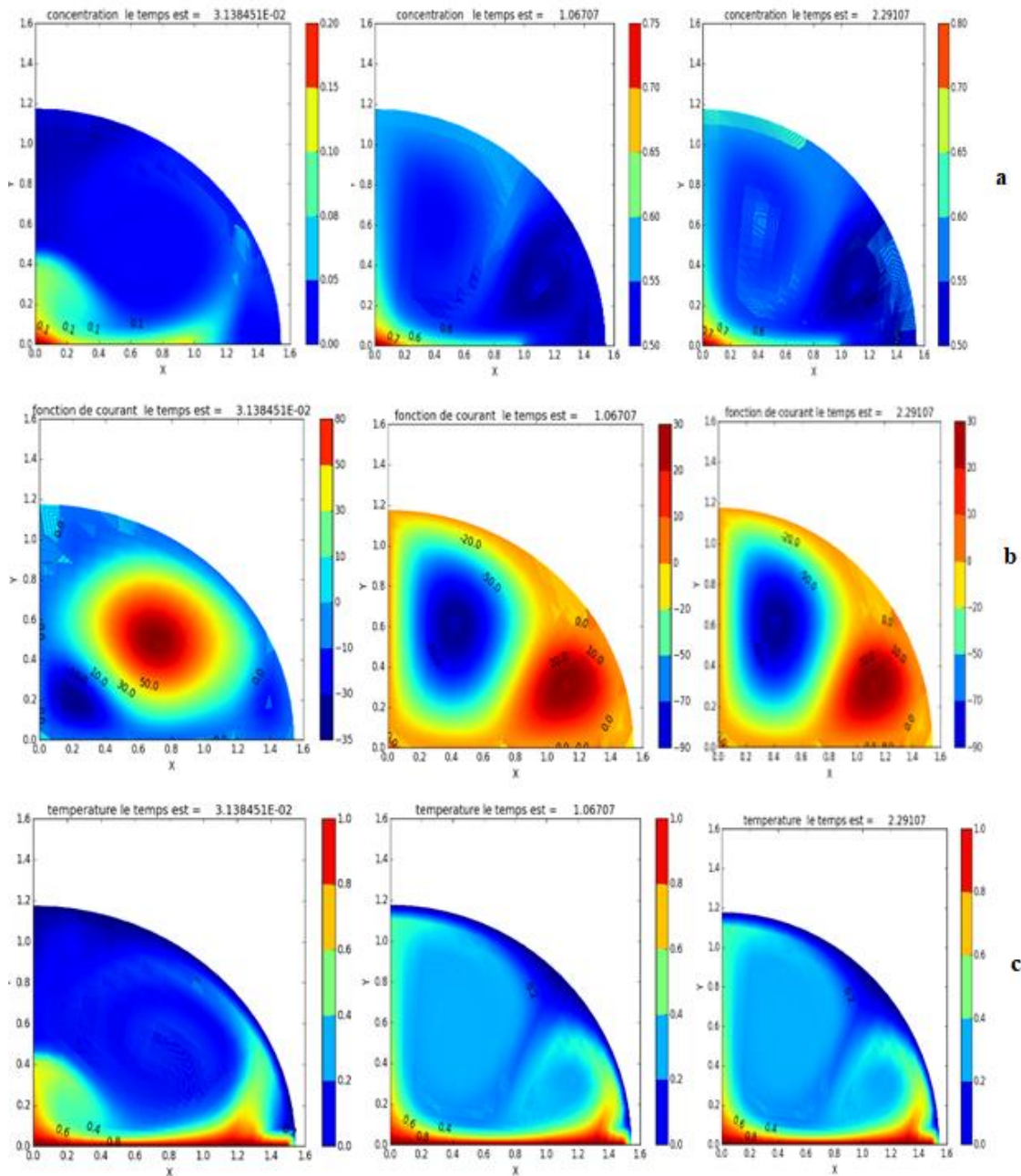
Fig.4 *Isoconcentration (a), streamlines (b) and isotherms (c) at different times for Rat=1.10^{+6} and Ram=0*

a. **Thermal field, current lines and iso concentration at variable times for $Rat = 1.10^{+6}$ and Ram =100,1000**

Figure 5 shows that the isotherms and iso-concentrations are almost parallel and concentric curves which denotes that for a low mass Rayleigh number Ram=100, mass transport in space is essentially controlled by the diffusion process. Fluid streamlines organize into two cells that rotate very slowly in opposite directions.

For Ram=1000, Figure 6 illustrates the fact that the isotherms and iso-concentrations transform and end up adopting the shape of a mushroom. We also note that, in this case, the distribution of temperatures and concentrations are different

When the mass Rayleigh number becomes important, Ram=1000, figures 5 and 6 show that the isotherms and iso-concentrations are more confined near the walls and that in the middle of space the values of these iso lines are almost constants in the upper half of the latter.

_____

Figure 5 shows that the isotherms and iso-concentrations are almost parallel and concentric curves which denotes that for a low mass Rayleigh number Ram=100, mass transport in space is essentially controlled by the diffusion process. Fluid streamlines organize into two cells that rotate very slowly in opposite directions.

For Ram=1000, Figure 6 illustrates the fact that the isotherms and iso-concentrations transform and end up adopting the shape of a mushroom. We also note that, in this case, the distribution of temperatures and concentrations are different.

When the mass Rayleigh number becomes important, Ram=1000, figures 5 and 6 show that the isotherms and iso-concentrations are more confined near the walls and that in the middle of space the values of these iso lines are almost constants in the upper half of the latter.
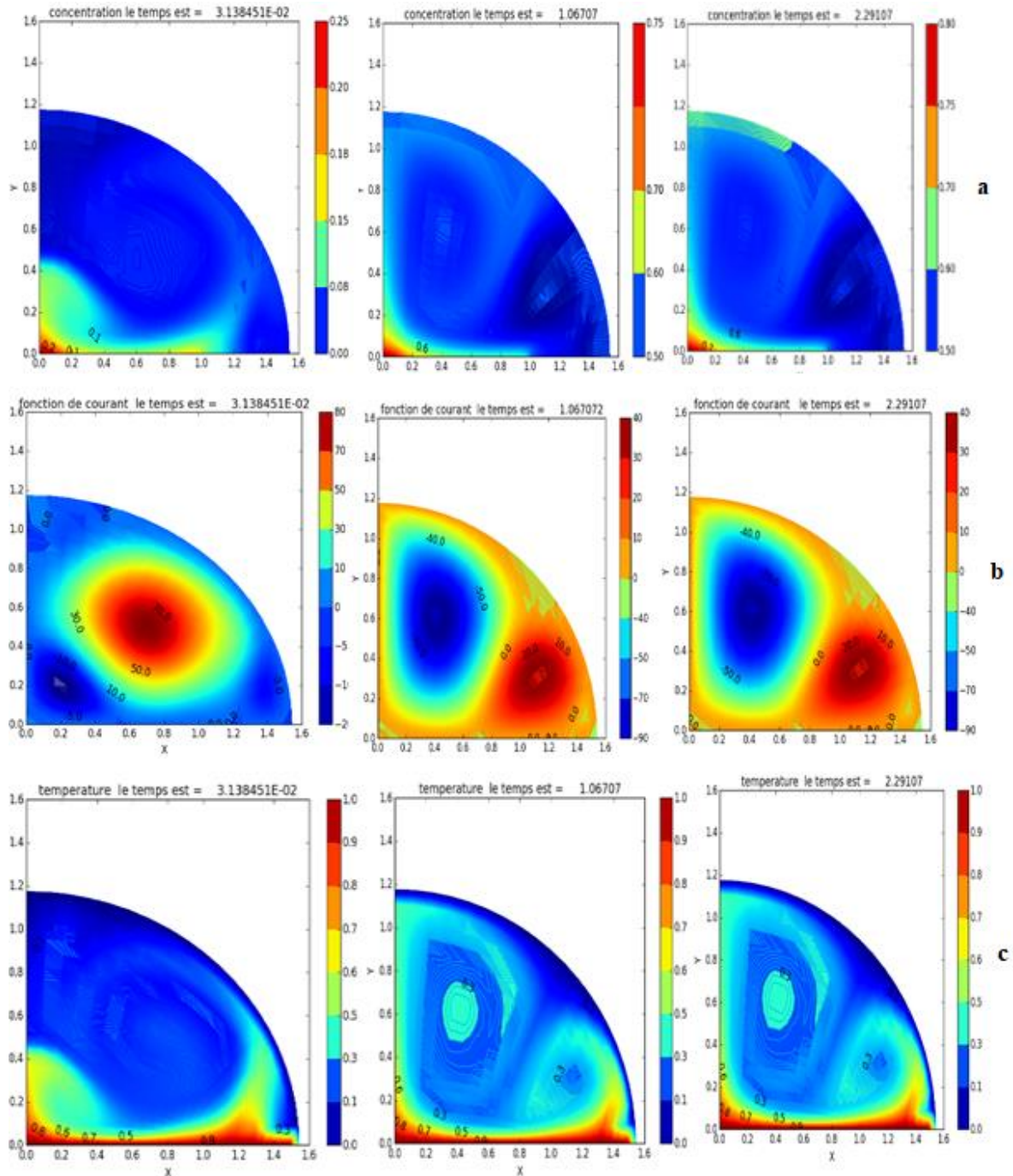

Fig.5 *Isoconcentration (a), streamlines (b) and isotherms (c) at different times for Rat=1.10^{+6} and Ram=100*
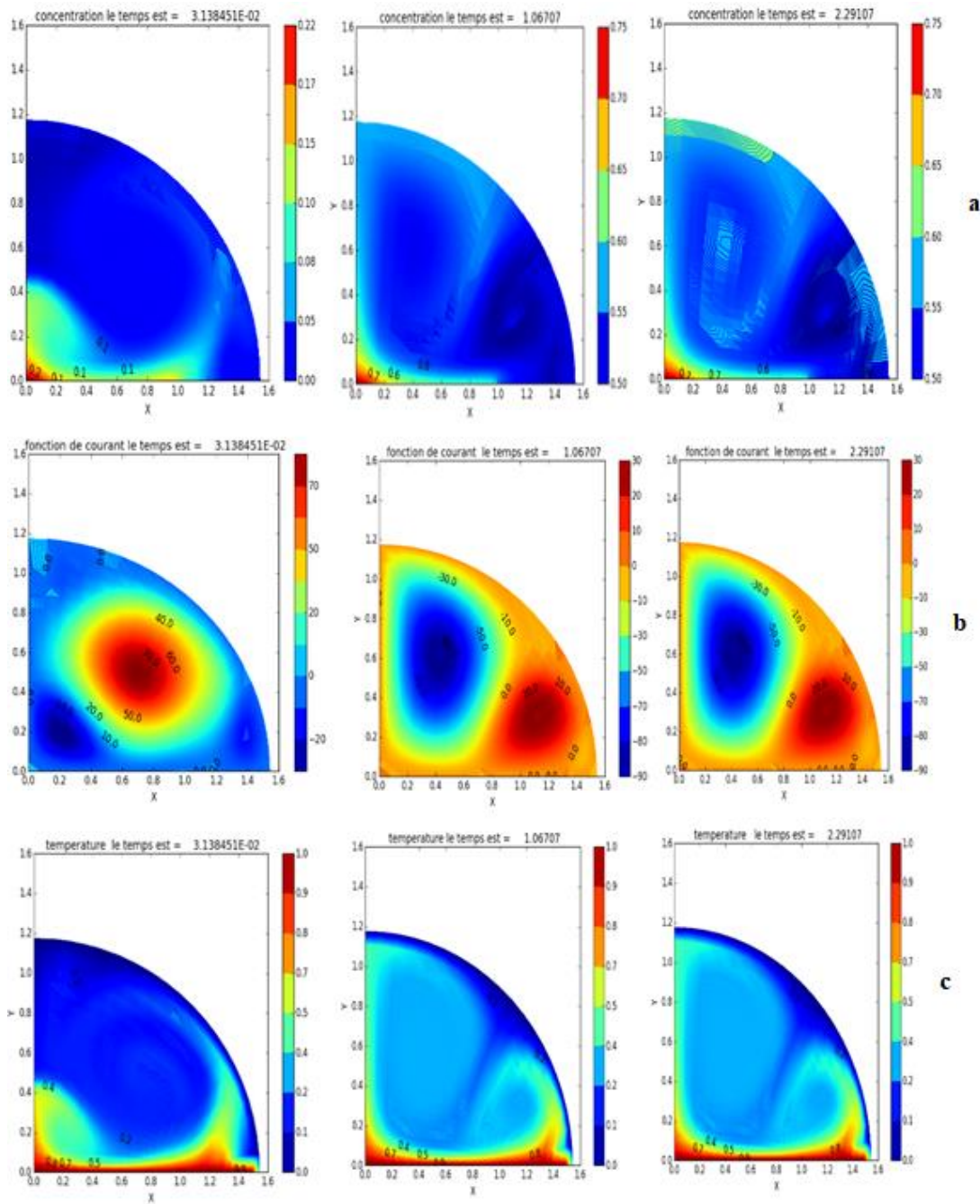
***Fig.6** Isoconcentration (a), streamlines (b) and isotherms (c) at different times for Rat=1.10^{+6} and Ram=1000*

Figures 4b, 5b and 6b show the streamlines for a form factor equal to 1 and for values of the mass Rayleigh number between 0 and 1000. According to these figures, the streamlines follow the shape of the front part of the plate, the flow not yet being disturbed. As the Reynolds number increases, the vorticity becomes more intense and moves closer to the bottom wall. This is simply explained by the fact of the importance of the fluid entry speed into the channel, the considerable narrowing of the channel at the level of the plate and obviously the adhesion of the fluid to the wall. Overall, the presence of the lower wall causes a disturbance of the flow in the channel. We represent in Figures 4c, 5c, 6c the curves which illustrate the isotherms for the same values of the thermal Rayleigh number, a heat flux of constant density having been imposed at the base of the lower wall. It can be noted that the greater the mass Rayleigh number, that is to say the higher the speed of the fluid, the more the heat is concentrated in the vicinity of the lower wall of the channel and in particular in the zone where the vortices reign. It should be noted that the heat flow injected at the base of the plate, the mass Rayleigh number does not influence the temperature distribution upstream of the obstacle because the heat transport takes place essentially by convection

CONCLUSION

In this part, after having validated the calculation code, we analyzed the results, the phenomenon of natural Rayleigh-Bénard convection within a binary fluid in a closed impermeable and non-catalytic enclosure delimited by a half cylinder, heated by its lower wall. The analysis was carried out for three mass Rayleigh numbers (Ram = 0, Ram = 100 and Ram = 1000). However, it should be noted that the model used in this study is two-dimensional for laminar flow. As natural flows are mostly turbulent, it would be interesting to confirm these results using a three-dimensional numerical model, in the context of turbulence, which could provide a good understanding of the physical phenomenon linked to flow with deposition as a whole. the problem of deposit deserves to be studied more closely. This document is devoted to the study of the phenomenon of natural Rayleigh-Bénard convection within a binary fluid in a closed impermeable and non-catalytic enclosure delimited by a half-cylinder. Thus, the validity limit of the two-dimensional flow was discussed based on the Rayleigh number and the ratio of thermal conductivities. The results showed that the structure of the flow as well as the average heat transfer is strongly influenced by the ratio of thermal conductivities, in the diffusive regime as in the convective regime. A multiplicity of solutions has been proven in the convective regime and the local distributions of temperature, Nusselt number and heat flux depend significantly on it.

NOMENCLATURE

C, Mass fraction of the species in the binary mixture
Cp Specific heat capacity [$J. kg^{-1}. K^{-1}$]
D, Molecular diffusion coefficient [$m^2. s^{-1}$]
g , Gravity field intensity [$N. kg^{-1}$]
h Metric coefficient [m]
l Plate length [m]
L Length of plate[m]
t, Dimensional time[s]
T, Binary fluid temperature[K]
T_{imp}, ource temperature [K]
v_η, Component according to η of the speed vector [m . s^{-1}]
v_θ, Component according to θ of the speed vecto [m . s^{-1}]
$\vec{v}$, Barycentric vector of the binary fluid
x,,Cartesian coordinate[m]
y,,Cartesian coordinate[m]
z, Cylindrical coordinate in axial direction [m]
T^*, Reduced temperature difference (dimensionless)
α,Thermal diffusivity[$m^2. s^{-1}$]
β_C, Mass expansion coefficient
β_T, Thermal expansion coefficient [K^{-1}]
δT, Reference temperature difference [K]
λ,Thermal conductivity[$W. m^{-1}. K^{-1}$]
μ, Dynamic viscosity [Pa. s]
v,Kinematic viscosity [$m^2. s^{-1}$]
ρ, , Fluid density fluide [$kg. m^{-3}$]
ρ_i,Density of species (i) in the mixture [$kg. m^{-3}$]
ψ,Current function [$m^2. s^{-1}$]
ω, Vorticity [s^{-1}]
η, Elliptical coordinate
θ, Elliptical coordinate
η_p, Component of η on the exterior wall

Gr_m,Mass Grashof number $Gr_m = \frac{g.\beta_c.L^3.\delta C}{(v_0)^2}$

Gr_t,Thermal Grashof number $Gr_t = \frac{g.\beta_T.L^3.\delta T}{(v_0)^2}$

Pe_m, Mass Péclet number $Pe_m = \frac{v_r.L}{D_0}$

Pe_t, Thermal Péclet number $Pe_t = \frac{v_r.L}{\alpha_0}$

Pr, Prandtl number $Pr = \frac{v_0}{\alpha_0}$,

Ra_m, Mass Rayleigh number $Ra_m = Gr_m. Pr = \frac{g\beta_T L^3 \delta C}{\alpha_0.v}$

___

Ra_T, Thermal Rayleigh number $Ra_T = Gr_t . Pr = \frac{g\beta_T L^3 \delta T}{\alpha_0 . v}$

Re, Reynolds number $Re = \frac{v_r 8.L.\rho_0}{\mu_0}$

REFERENCES

[1]. G. De Vahl Davis, Natural convection of air in a square cavity, a benchmark numerical solution, Int. J. Numer. Methods Fluid 3 (1962), 249-264.

[2]. A. Diouf, O. Dramé and M. N. Koïta, Numerical simulation of a natural convection of air between two square cavities for different Rayleigh values with a constant magnetic field, Journal of Chemical, Biological and Physical Sciences (JCBPS) : Section C 12(1) (2021), 034-039.

[3]. H. Q. Yang, K. T. Yang and Q. Xia, Periodic laminar convection in a vertical cavity, Int. J. Heat and Mass Transfer 32(11) (1989), 2199-2207.

[4]. M. K. Kane, C. Mbow, M. L. Sow and J. Sarr, Numerical simulation of two dimensional natural convection in a confined environment with the vorticitystream function formulation, Open Journal of Fluid Dynamics 8 (2018), 44-58.

[5]. K. C. Karki and P. S. Sathyamurthy, Laminar mixed convection in a horizontal semi-circular duct with axially, Int. J. Heat and Mass Transfer 25 (1994), 171-189.

[6]. T. H. Kuehn and J. Goldstein, An experimental study of natural convection heat transfer in concentric and eccentric horizontal cylindrical annuli, ASME J. Heat Transfer 100 (1978), 635-640.

[7]. Y. N. Lee and W. J. Minkowycz, Heat transfer characteristics of the annulus of tow-axial cylinders with one cylinder rotating, Int. J. Heat and Mass Transfer 4(32) (1989), 711-722.

[8]. R. M. Abd-Elwahed, A. E. Attia and M. A. Hifni, Experiments on laminar flow and heat transfer in an elliptical duct, Int. J. Heat and Mass Transfer 27 (1984), 2397-2413.

[9]. V. D. Sakalis, P. M. Hatzikonstantinou and N. Kafousias, Thermally developing flow in elliptic ducts with axially variable wall temperature distribution, Int. J. Heat and Mass Transfer 45 (2002), 25-35.

[10]. M. N. Borjini, Ch. Mbow and M. Daguenet, Numerical analysis of the effect of radiation on laminar steady natural convection in a two-dimensional participating medium between two horizontal confocal elliptical cylinders, 35 (1999), 467-494. Natural Unsteady Thermal Convection in a Space ... 105

[11]. M. M. Elshamy, M. N. Ozisik and J. P. Coulter, Correlation for laminar natural convection between con focal horizontal elliptical cylinders, Numer. Heat Transfer, Part A 18 (1990), 95-112.

[12]. M. Rahnama and M. Farhadi, Effect of radial fins on two-dimensional turbulent natural convection in horizontal annulus, International Journal of Thermal Sciences 43 (2004), 255-264.

[13]. S. M. El-Sherbiny and A. R. Moussa, Effects of Prandtl number on natural convection in horizontal annular cavities, Journal of Alexandria Engineering 43 (2004), 561-576.

[14]. M. Djezzar and M. Daguenet, Natural steady convection in a space annulus between two elliptic confocal ducts: influence of the slope angle, Journal of Applied Mechanics Transaction of the ASME 72 (2006), 88-95.

[15]. H. C. Topakoglu and O. A. Arnas, Convective heat transfer for steady laminar flow between two confocal elliptic pipes with longitudinal uniform wall temperature gradient, Int. J. Heat and Mass Transfer 17 (1974), 1487-1498.

[16]. Y. D. Zhu, C. Shu, J. Qiu and J. Tani, Numerical simulation of natural convection between two elliptical cylinders using DQ method, Int. J. Heat and Mass Transfer 47 (2004), 797-808.

[17]. Ucheul Shin, Joseph Khedari and Cheikh Mbow, Michel Daguenet, Etude théorique de la convection thermique à l'intérieur d'une calotte cylindrique d'axe horizontal, Int. J. Heat and Mass Transfer 37 (1994), 2007-2016.

[18]. Z. Kabdi, U.-Ch. Shin, Ch. Mbow and M. Daguenet, Convection thermique naturelle laminaire, permanente et bidimensionnelle dans des lunules cylindriques, Rev. Gen. Therm. 36 (1997), 319-329.

[19]. S. V. Patankar, Numerical Heat Transfer and Fluid Flow, McGraw-Hill Book Company, New York, 1980.

[20]. Mariama Néné Koita, Mamadou Lamine Sow, Omar Ngor Thiam, Vieux Boukhaly Traoré, Cheikh Mbow and Joseph Sarr, Unsteady natural convection between two eccentric hemispheres, Open Journal of Applied Sciences 11 (2021), 177-189.

[21]. P. J. Roache, Computational Fluid Dynamics, Hermosa, New York, 1982.

[22]. H. K. Versteeg and W. Malalasekera, An Introduction to Computational Fluid Dynamics: The Finite Volume Method, John Wiley and Sons Inc., NY, 1995